Development of an Autonomous Magnetic Permeability Sensor

Polychronis Pattakos[1], Angelos Katsoulas[1], Spyridon Angelopoulos[1], Aphrodite Ktena[2], Panagiotis Tsarabaris[1], and Evangelos Hristoforou[1]

[1]School of Electrical and Computer Engineering, National Technical University of Athens, 15780 Athens, Greece
[2]General Department, National and Kapodistrian University of Athens, 15784 Athens, Greece

In our days, there is an undeniable need for control over the quality of metals in machines, metal components, tools, and construction materials during production and maintenance. Nondestructive testing sensors have been proven to be the most effective way of determining the quality of the composition of materials since they can detect flaws, not only during their construction but also during maintenance, without interfering with, or obstructing, their use. This article focuses on the measurement of the magnetic permeability of ferromagnetic steels and alloys as a nondestructive method of correlating magnetic properties with residual stresses based on the use of a yoke-shaped sensor. Most importantly, an electromagnetic energy harvesting system has been designed and tested, based on the exploitation of mechanical vibrations. The combination of the sensor and the energy harvesting system can lead to an energy autonomous device, which can be placed in inaccessible locations for remote nondestructive testing where measurements can be taken and transmitted autonomously every 10 min. Said transmission is realized by a network of yoke sensors in multiplex configuration and sent to a central sensor, leading to an Internet of Things usable device.

Index Terms—**Energy harvesting, Internet of Things, magnetic permeability, nondestructive testing.**

I. Introduction

IN TODAY'S world where the Internet of Things is the new standard for industrial applications [1], there is much motive and also opportunity for rethinking traditional methods and devices of measuring the properties of materials used during their production, use, or maintenance. Nondestructive testing [2] continues to be the most efficient way, but the sensors used in such measurements have to be redesigned in order to meet the new specifications. This article describes the process of building a magnetic permeability sensor and then redesigning it for autonomous operation through energy harvesting.

II. Magnetic Permeability

Magnetic permeability (represented by μ) is generally defined as the ratio of the magnetic flux density $\boldsymbol{B}$ inside a given material and the effective magnetic field $\boldsymbol{H}$ experienced by it, as shown in the following:

$$\boldsymbol{B} = \mu \cdot \boldsymbol{H}. \tag{1}$$

The effective magnetic field $\boldsymbol{H}$ experienced by a given magnetic volume is the applied field minus any demagnetizing fields. The magnetic permeability of ferromagnetic materials is a function of $\boldsymbol{H}$ and orders of magnitude greater than μ_0, the permeability of free space. Hence, it can be used as a measure of the quality of a magnetic material. Compared to a flawless, homogeneously magnetized material, the presence of defects results in lower induction $\boldsymbol{B}$ and, hence, lower permeability μ, for a given effective field value.

Manuscript received 22 June 2022; revised 16 August 2022; accepted 1 September 2022. Date of publication 8 September 2022; date of current version 26 January 2023. Corresponding author: E. Hristoforou (e-mail: hristoforou@ece.ntua.gr).

Color versions of one or more figures in this article are available at https://doi.org/10.1109/TMAG.2022.3205106.

Digital Object Identifier 10.1109/TMAG.2022.3205106

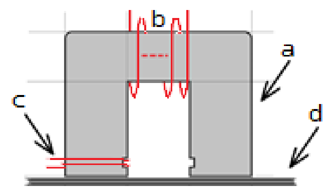

Fig. 1. Magnetic permeability sensor.

For practical purposes, as well as in the arrangement proposed in Section III, the quantity measured is the so-called differential magnetic permeability μ_D, which is defined as $\mu_D = (dB/dH)$, where B and H are measured along the same direction.

For ferromagnetic materials, the value of μ is much greater than that of free space, which makes the magnetic field created within them much stronger than the one created in free space or air. Using this principle, it is easy to detect flaws in components made of ferromagnetic materials, as the induced magnetic field within them will be much weaker than expected, compared to a component that is flawless.

III. Magnetic Permeability Sensor

A. Design

The magnetic permeability sensor (Fig. 1) realizes three quarters of a magnetic circuit with the specimen completing it [3].

The sensor consists of three main parts: (a) a yoke-shaped core, a primary coil (b: Coil A) that acts as a source of magnetic flux, and a secondary coil (c: Coil B) that acts as a receiver of the magnetic density. The air gaps between the specimen (d) and the yoke have to be considered while measuring.

The equivalent magnetic circuit is shown in Fig. 2. $\boldsymbol{F}_1$ and $\boldsymbol{F}_2$ are the magnetomotive forces of coils A and B, respectively, R_{g1} and R_{g2} are the magnetic reluctances of the two air gaps, R_y and R_m are the magnetic reluctances of the core and the specimen, and $\boldsymbol{\Phi}$ is the circuit's magnetic flux.

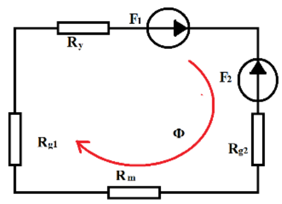

Fig. 2. Magnetic permeability sensor's equivalent magnetic circuit.

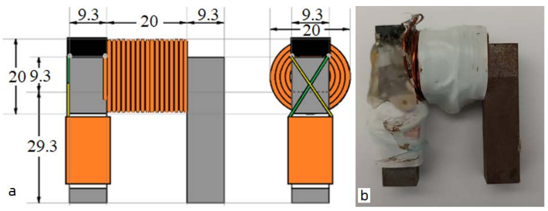

Fig. 3. (a) Mechanical schematic (dimensions in mm). (b) Actual image of the magnetic permeability sensor.

The core is made of typical electrical steel, used in transformers. Coil A is made of Ø1 mm insulated wire, has a total length of 20 mm, and consists of 68 turns. Coil B is made of Ø0.1 mm wire, has a total length of 18 mm, and consists of 150 turns.

As the magnetic permeability sensor [Fig. 3(b)] may be used as part of a bigger structure, it is important that its results can be replicated. Thus, a second sensor (referred to as Sensor II) was constructed using the physical properties of the first [Fig. 3(a)]. The two sensors (Table I) were tested for calibration, and then, their experimental results were compared.

B. Circuitry

The magnitudes of the magnetic field H and the magnetic flux density B are given in [4] as

$$H = \frac{N_1}{Z_1 \cdot l_1} \cdot V_1 \tag{2}$$

$$B = \frac{1}{N_2 \cdot S} \cdot \int V_2 \cdot dt \tag{3}$$

where N_1 is the number of coil turns, Z_1 is the impedance, l_1 is the length, V_1 is the electric potential difference of Coil A, S is the cross-sectional area, N_2 is the number of coil turns, and V_2 is the electric potential difference of Coil B. Equations (2) and (3) show that H is proportional to V_1, whereas B is proportional to the integral of V_2, so an integrator circuit must be implemented to the output signal of Coil B, in order for the hysteresis loop to be formed on the oscilloscope (Fig. 4). With N_1, N_2, Z_1, l_1, and S being known quantities, (1) gives us the magnetic permeability. By definition [4], and through (2) and (3), we get the differential magnetic permeability μ_D, which is proportional to the output V_2, as seen in (4), and is more useful to consider, especially for nonlinear magnetic materials

$$\mu_D := \frac{dB}{dH} = \frac{Z_1 \cdot l_1}{N_1 \cdot N_2 \cdot S} \cdot \frac{V_2}{dV_1/dt}. \tag{4}$$

C. Typical Measurements

A variety of samples was initially measured in the lab to test the functionality of the magnetic permeability sensor. Both Sensors I and II were used, in order to test their calibration. As indicative of the magnetic permeability of the samples, the peak-to-peak and rms values are measured (Table II).

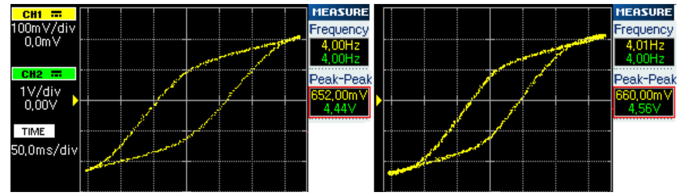

Fig. 4. Hysteresis loops of Sensors I and II for Sample A.

TABLE I
CHARACTERISTICS OF SENSORS

Sensor *I*	L_S	R_s
Coil A	318 μH	0.15 Ω
Coil B	2.11 mH	16.37 Ω
Sensor *II*	L_S	R_s
Coil A	298 μH	0.09 Ω
Coil B	1.98 mH	16.88 Ω

TABLE II
MEASUREMENT RESULTS

Load	**Sensor**	**Peak-to-Peak**	**RMS**
Steel Sample A	***I***	4.44 V	1.586 V
	II	4.56 V	1.628 V
Steel Sample B	***I***	4.56 V	1.628 V
	II	4.68 V	1.671 V
Steel Sample C	***I***	4.60 V	1.643 V
	II	4.68 V	1.671 V

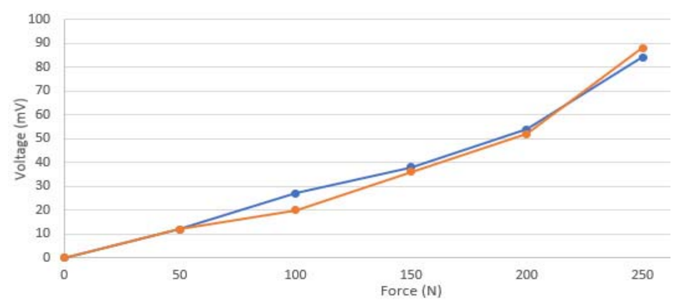

Fig. 5. Sample A's measurements graph.

D. Stress Measurements

Furthermore, tensile stress was applied to the sample, measured by a force gauge meter. The sensor was placed on the sample and rms measurements are taken (Fig. 5; Sensor I—blue, offset: +1583 V; Sensor II—orange, offset: +1628 V).

E. Construction of the New Sensor

In order to meet the specifications of an autonomous magnetic permeability sensor, a new sensing element had to be designed. The core is made of *Metglas*, replacing the original common electrical steel material. *Metglas* is also known as a metallic glass alloy, which differs from traditional metals in its noncrystalline structure and possesses unique physical and magnetic properties. It is made using rapid solidification which creates unique ferromagnetic properties along with very low core losses and very high relative permeability [5]. This particular part is the *AMCC-16B* made by Hitachi Metals, Ltd., and sold in pairs as to form a core of a transformer (Fig. 6), but only one half is used in this application.

In order for the sensor to work at low currents, new coils had to be constructed that would also fit the geometry of

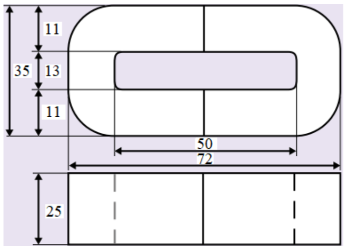

Fig. 6. Mechanical schematic of Metglas Core. Mass is 281 g. All dimensions are in mm [5].

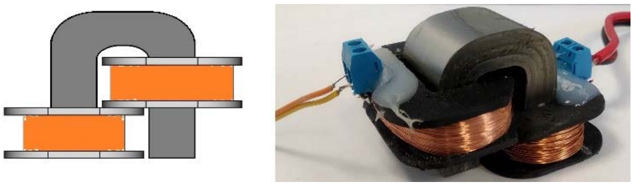

Fig. 7. Finished magnetic permeability sensor with Metglas Core.

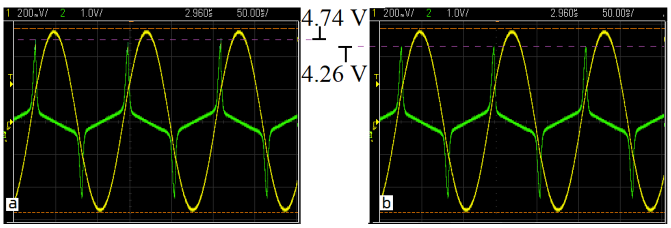

Fig. 8. Output for (a) flawless and (b) flawed part of the specimen.

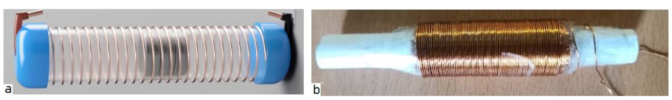

Fig. 9. (a) 3-D rendering. (b) Microgenerator with inertial mass inside the coil.

the new core. A set of bobbins had to be designed and 3-D printed so that the coils could be winded around. Coil A was made of 130 turns of Ø0.5 mm insulated wire and rates at 1.7 mH and 1.4 Ω. Likewise, Coil B was made of 2000 turns of Ø0.1 mm insulated wire and rates at 612 mH and 516 Ω. The two bobbins were placed with each one occupying one leg of the core (Fig. 7).

Measurements on a specimen with a flawless and a damaged part showed a very clear difference in output at 9 Hz and with an input of 0.57 V. Indicative peak-to-peak measurements were 4.74 V for the flawless and 4.26 V for the flawed part (Fig. 8).

IV. Energy Harvesting System

A. System Description

The energy harvester is comprised of the generator and the energy storing circuit, connected through a power management circuit [6]. The generator used is one where an inertial mass of permanent magnets is placed inside a tube wrapped in a coil and is allowed to levitate inside the tube by placing two magnets of opposite polarity on each side (Fig. 9).

When the external vibrations are applied, the magnets begin to oscillate inside the tube, creating a differential magnetic field inside the coil, which results in alternating voltage at the coil's edges [5]. According to [7], such a system can be represented by an electrical circuit equivalent. Fig. 10 shows the circuit equivalent of the generator.

Here, m is the inertial mass of the generator, s is the external vibration, $Y(s)$ is the oscillation caused by the external force,

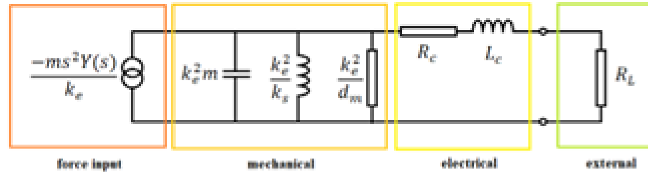

Fig. 10. Circuit equivalent of electromagnetic microgenerator.

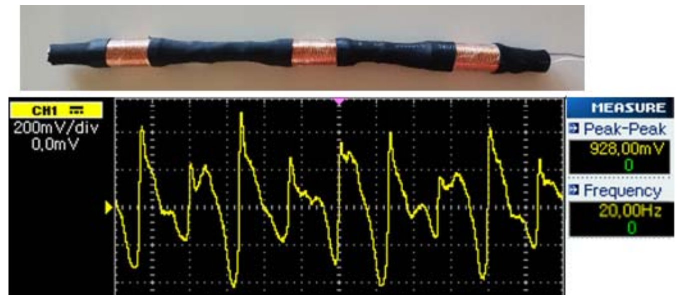

Fig. 11. Three generator system and its voltage output at 20 Hz [6].

k_e is the factor of convection that is particular to the system, k_s is the system's elastic properties factor, d_m is the mechanical damping factor, R_c is the generator's internal resistance, L_c is the generator's internal inductance, and R_L is the external load. To achieve maximum efficiency, six design conditions were followed, which are derived from the circuit analysis on the above circuit equivalent [7].

1) Inertial mass of the magnet must be the largest possible.
2) The system's elastic factor must be chosen so that the resonant frequency of the inertial mass is as close as possible to the frequency of the external oscillation.
3) The geometry of the generator must account for enough space for oscillation of the inertial mass.
4) The internal resistance of the generator R_c must be at least one order of magnitude less than that of the load.
5) Mechanical damping must be as little as possible.
6) Electromagnetic constant k_e must be such that the internal resistance of the generator is as close as possible to the resistance of the load ($R_L \approx k_e^2/d_m$).

A plastic cylinder was chosen as shell for the permanent magnets that would act as inertial mass to oscillate inside it and also for the coil to be wrapped around. Neodymium (NdFeB) permanent magnets were chosen because of their strong magnetic field and high density. Two additional neodymium magnets were placed in fixed positions at the edges of the shell to ensure the most efficient oscillation inside the tube.

In the end, three microgenerators in series were used, two of which were 50 mm in length with 600 turns and with a total of 20 magnets of 10 mm diameter acting as inertial mass. The third was of the same characteristics except for the magnets that were 8 mm in diameter, in order to exploit a wider range of oscillating frequencies [6]. The three-generator system and its output can be seen in Fig. 11.

In order for the harvested energy to be stored, it must first be rectified. Generally speaking, diodes used in rectifiers can have a significant voltage drop so, in order to minimize their effect, it is first necessary to raise the alternative voltage through a transformer. Four identical Schottky diodes were used with a voltage drop of 150 mV for currents of up to 2 A. Energy

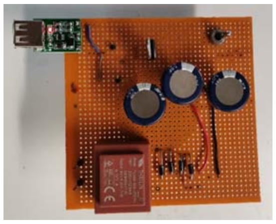

Fig. 12. Power management, storage, and output circuits prototype.

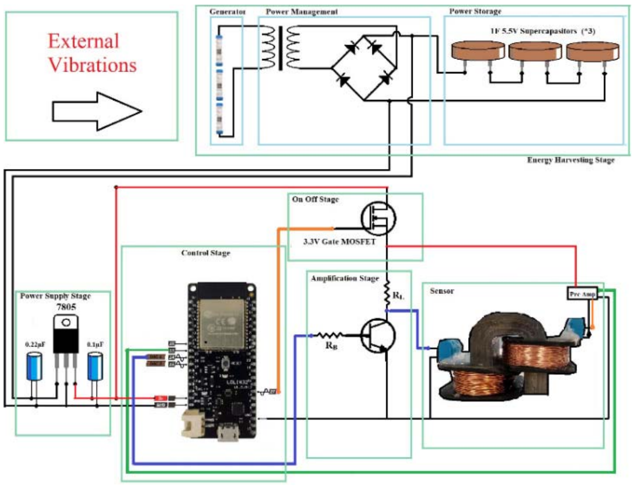

Fig. 13. Full system overview.

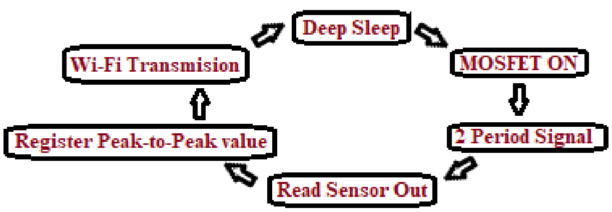

Fig. 14. Operation block diagram.

is stored using three supercapacitors of 1 F, 5.5 V connected in series (Fig. 12). This is equivalent to one 1/3 F, 16.5 V capacitor, and the nominal total storable energy is $E = 45.3$ J (using $E = C \times V^2/2$). During the experiment, the capacitors reached 14 V, so the storable charge is 4.7 C and the actual energy stored is 32.6 J. Experimental data [6] show that 20 min is enough for such energy in the form of charge to be having completely empty capacitors at the beginning.

V. Autonomous Magnetic Permeability Sensor

A. General Description

The autonomous magnetic permeability sensor system can be seen in Fig. 13.

In addition to features presented above, an *ESP32* Microcontroller was used to control the application, connected to a MOSFET for ON–OFF control and also creating a signal that is then amplified and send to the sensor. *ESP32* was chosen for its in-built Wi-Fi chip, its low power consumption, and its ability to switch to deep sleep mode. This particular version is the *ESP32 WeMos LOLIN 32* breakout board, which comes with the extra feature of battery monitoring [8]. The block diagram is shown in Fig. 14.

ESP32 has nominal operating currents of 10 μA during deep sleep and 260 mA during normal operation at 3.7 V, so it can be calculated that a full cycle of 10 min with only 0.5 s of operation consumes no more than 0.5 J. Likewise, having the sensor operating for 0.5 s at $V = 0.571 \times \sin \omega t + 0.571$ V has a consumption of 0.16 J. The rest of the circuit's energy consumption, which includes the MOSFET, the amplification transistor, and the preamp which is based on the *NE5534* chip [9] along with the heat dissipation on the resistors, can also be calculated to be less than 2 J due to the very small period of operation. In total, each 10 min cycle has a maximum energy consumption of less than 2.7 J. Given that the total amount of energy stored is 32.6 J and the full charging time was 20 min, it is shown that the system can work autonomously.

VI. Conclusion

Nondestructive testing seems to be an ideal match for new Internet of Things applications like this. The development of new materials used for building sensing elements and energy storage along with the ease of access to new interconnected electronics shows great prospects for magnetic sensors to be redesigned based on current industrial needs. The autonomous magnetic permeability sensor described in this article serves not only as a proof of concept for measuring magnetic permeability but also as a new template for energy harvesting along with data transmission to be implemented on other IoT sensors. It is important to note that magnetic permeability sensors used in nondestructive testing are very specific to the geometry and other physical qualities of the subject that is being tested or monitored. The principles that have been implemented when designing the autonomous magnetic permeability sensor have to be reexamined when implemented in a new application.

Acknowledgment

This work was supported by the European Union and Greek National Funds through the Operational Program Competitiveness, Entrepreneurship and Innovation, under the call RESEARCH-CREATE-INNOVATE under Project T2EDK-02521.

References

[1] D. P. Acharjya and M. K. Geetha, *Internet of Things: Novel Advances and Envisioned Applications*. Berlin, Germany: Springer, 2017.

[2] L. Cartz, *Nondestructive Testing*. Chennai, Tamil Nadu: ASM International, 1995.

[3] E. M. Purcell, *Electricity and Magnetism*. New York, NY, USA: McGraw-Hill, 1985.

[4] P. Pattakos, "Development of magnetic permeability sensor," M.S. thesis, Dept. Elect. Comput. Eng., Nat. Tech. Univ. Athens, Athens, Greece, 2019. [Online]. Available: http://dspace.lib.ntua.gr/handle/123456789/48863

[5] Hitachi Metals. (2017). *Metglas? AMCC Series Cut Core, Power Electronics Components Catalog*. Accessed: Jun. 20, 2022. [Online]. Available: https://www.hitachimetals.com/materials-products/amorphous-nanocrystalline/powerlite-c-cores/documents/AMCC-F3CC-series-Cut-Cores_hl-fm27-c.pdf

[6] A. Katsoulas, "Development of a magnetic system for energy harvesting from vibrations in ships," M.S. thesis, Dept. Electr. Comput. Eng., Nat. Tech. Univ. Athens, Athens, Greece, 2022.

[7] C. B. Williams, "Development of an electromagnetic micro-generator," *IEEE Proc. Circuits Devices Syst.*, vol. 148, no. 6, pp. 337–342, Jan. 2002.

[8] Renzo Mischianti. (Dec. 1, 2021). *ESP32 WEMOS Lolin32 High Resolution Pinout and Specs*. Accessed: Jun. 20, 2022. [Online]. Available: https://www.mischianti.org/2021/02/21/esp32-wemos-lolin32-high-resolution-pinout-and-specs/

[9] *Dual and Single Low Noise op Amp*, Philips [NXP Semiconductors], Eindhoven, The Netherlands, datasheet NE5533/5533A/NE/SA/SE5534/5534A, Aug. 1994.